ELSEVIER

Journal of Chromatography B, 720 (1998) 153–163

JOURNAL OF CHROMATOGRAPHY B

Evidence for the denaturation of recombinant hepatitis B surface antigen on aluminium hydroxide gel

Dina Tleugabulova[a,*], Viviana Falcón[b], Eduardo Pentón[c]

[a]*Quality Control Department, National Center for Bioproducts, P.O. Box 6048, Havana 6, Cuba*
[b]*Department of Physical Chemistry, Center for Genetic Engineering and Biotechnology, P.O. Box 6162, Havana, Cuba*
[c]*Vaccine Division, Center for Genetic Engineering and Biotechnology, P.O. Box 6162, Havana, Cuba*

Received 11 March 1998; received in revised form 15 August 1998; accepted 8 September 1998

Abstract

Despite the complexity of the subject of protein–alum interactions, a valuable information can be obtained by analyzing the adsorbed and desorbed protein by common physico–chemical methods. In the present work, to approach the adsorption of hepatitis B surface antigen (HBsAg) on alum, the experimental data were supported by complementary analyses of the adsorbed protein by immunoelectron microscopy and the desorbed protein by denaturing size-exclusion chromatography and sodium dodecyl sulfate-polyacrylamide gel electrophoresis under reducing conditions. First, the depletion of HBsAg was investigated. The aspects assessed were the conditions, recovery and chromatographic performance of the desorbed protein. The results obtained strongly suggested the loss of particulate structure of HBsAg after adsorption on alum. This conclusion was further reinforced by direct immunoelectron microscopic visualization of HBsAg in the adsorbed state.

Keywords: Hepatitis B surface antigen; Aluminium hydroxide

1. Introduction

According to World Health Organization estimates, by the year 2000, there will be 400 million hepatitis B virus carriers in the world if hepatitis B vaccine is not widely used [1]. Several yeast-derived hepatitis B vaccines are commercially available now based on the same recombinant hepatitis B surface antigen (HBsAg) and aluminium hydroxide (alum) adjuvant. In numerous clinical trials, these preparations have demonstrated an immunogenicity and efficacy similar to that of plasma-derived antigen, with no difference in antibody specificity and avidity [2–4]. However, using both plasma- and yeast-derived vaccines, a small portion (about 5–10%) of vaccinated subjects fail to produce detectable antibody response. Induction of immune reactivity depends upon antigen reaching and being available in lymphoid organs in a dose- and time-dependent manner [5]. Since HBsAg is administered as the alum-adsorbed preparation, antigen–alum interactions should be crucial in the immune response. This was experimentally shown for gp120 protein [6]. As most proteins, gp120 is quantitatively adsorbed on alum in a few minutes. However, the gp120–alum interaction is weak and sensitive to anions from physiological fluids. Due to this, the protein is rapidly desorbed from alum just after injection that

*Corresponding author.

0378-4347/98/$19.00
PII: S0378-4347(98)00425-3

explains a weak immune response to the MN gp120 HIV-1 vaccine.

Our understanding of antigen–alum interactions may provide a way to understand the non-responsiveness of some people to hepatitis B vaccination. The analysis of antigen–alum interactions requires knowledge of both the kinetic events that occur during the adsorption event and the structure of adsorbed protein. However, neither of these aspects has been explored for alum-adsorbed proteins due to the lack of reliable experimental techniques capable to support kinetic measurements as well as to assess the adsorbed protein at a molecular level [Review, 7]. Despite the complexity of alum structure [8] and great structural variety among antigens, protein adsorption on alum is commonly approached by Langmuir model originally developed for small molecules adsorbing at an 'ideal' surface. This model cannot describe the adsorption behavior of several antigen proteins [9], including HBsAg [unpublished results]. However, without the stimulus of usable data, no superior theoretical treatment has been developed.

Despite the complexity of the subject of protein–alum interactions, a valuable information can be obtained by analyzing the adsorbed and desorbed protein by common physico–chemical methods. In the present work, to approach the adsorption of hepatitis B surface antigen (HBsAg) on alum, the experimental data were supported by complementary analyses of the adsorbed protein by immunoelectron microscopy and the desorbed protein by denaturing size exclusion chromatography (SEC) and sodium dodecyl sulfate-polyacrylamide gel electrophoresis (SDS-PAGE). The results obtained evidence the loss of particulate structure of HBsAg after adsorption on alum. The same has been previously suggested from the immunological studies of HBsAg [10] and another virus-like particles [11,12]. Hence, our work provides a physico–chemical support to this hypothesis.

2. Experimental

2.1. Materials

Tris(hydroxymethyl)aminomethane, dithiotreitol (DTT), SDS, mercaptoethanol, sodium chloride, sodium phosphates and another mentioned reagents were analytical grade and obtained from Merck (Darmstadt, Germany). The reagents used in electron microscopy were from Agar Scientific (Essex, UK). All solutions were made in Milli-Q grade water. Aluminium hydroxide gel (alum) was purchased as a sterile 2% (w/v) $Al(OH)_3$ suspension from Superfos Biosector (Vedbaek, Denmark). Hyflo Super Cel (celite) was from Fluka (Buchs, Switzerland). Phosphate-buffered saline (PBS) contained 1.7 m*M* KH_2PO_4, 7.9 m*M* Na_2HPO_4, 2.7 m*M* KCl and 250 m*M* NaCl, pH 7.0. Recombinant HBsAg, cloned and expressed in yeast *Pichia pastoris*, was purified by a multi-step procedure [13] and provided as a solution in PBS (1.61 mg/ml) from the National Center for Bioproducts (Havana, Cuba). This stock solution was used in the preparation of working standard solutions of lower concentrations as well as in the adsorption studies.

Anti-HBsAg mouse monoclonal antibody (CB Hep1) and protein A–colloidal gold complex (particle diameter, 15 nm) used for the immunodetection of HBsAg were provided by the Division of Immunotechnology and Diagnostics of the Center for Genetic Engineering and Biotechnology (Havana, Cuba).

The HBsAg–celite preparation (100 μg/ml HBsAg) used as a reference standard in the electron microscopic study of HBsAg–alum preparation was prepared as described in Ref. [14].

2.2. Apparatus

2.2.1. Size-exclusion chromatography (SEC)

The SEC system included a Pharmacia LKB 2248 pump, Knauer degasser, Pharmacia 2141 variable-wavelength UV detector operated at 280 nm and Pharmacia 2221 programmable integrator. The column used was a TSK G4000 SW (600×7.5 mm I.D.) purchased from Tosohaas (Stuttgart, Germany). Elution was with 0.1 *M* Tris–HCl in 0.3% SDS, pH 8.0 at 0.9 ml/min. After injecting the working standard solutions (100 μl), the conversion of peak areas to protein concentrations was carried out using programmable integration.

2.2.2. SDS-PAGE

Electrophoresis (Hoefer Scientific Instrument) was performed as described by Laemmli [15] on 12.5%

gels at 30 mA for 3.5 h at room temperature under reducing conditions. The gels were stained by Coomasie blue dye (Bio-Rad, Richmond, CA, USA) or silver nitrate [16]. The Coomasie-stained gel was scanned by laser densitometry using Ultroscan XL (Pharmacia). For immunoblotting, the gel was incubated with CB Hep1 antibody and developed with protein A conjugated to aminobenzidine [17].

2.3. Preparation of HBsAg–alum

A mixture of 2% aluminium hydroxide gel (2 ml) and HBsAg stock solution (1.7 ml) was gently agitated for 30 min at room temperature and then diluted with PBS in a 25-ml volumetric flask. The concentration of adsorbed HBsAg was 100 μg/ml, as determined by Lowry method [18] from protein balance. The placebo was prepared by the dilution of 2% aluminium hydroxide gel (2 ml) with PBS up to 25 ml.

2.4. Reduction of HBsAg particles

Aliquots (200 μl) from working standard solutions (0.2–1.6 mg/ml HBsAg) were incubated with DTT/M sample buffer (40 μl) for 10 min at 100°C [The DTT/M sample buffer contained 417 m*M* DTT, 4.2% (w/v) SDS and 16% 2-mercaptoethanol]. The reduced samples were analyzed by SDS-PAGE/Coomasie blue staining (30 μl) and SEC (100 μl) as described.

2.5. Desorption of HBsAg from alum

One ml of the HBsAg–alum preparation (100 μg/ml) was centrifuged for 10 min at 2500 rpm. The pellet separated was incubated for 3 min at 100°C with a mixture of 0.4 *M* Na/PO_4, pH 8.0 (100 μl)–DTT/M sample buffer (20 μl) (5:1). After centrifugation for 5 min at 10 000 rpm, the supernatant was analyzed by SDS-PAGE/Coomasie blue staining (30 μl) and SEC (100 μl).

In order to determine the HBsAg recovery after desorption, the area of SEC-peak from the desorbed sample was extrapolated to the calibration curve previously generated by injections of the HBsAg working standard solutions. The determinations were carried out in duplicate.

In another experiment (Fig. 5), the HBsAg was desorbed from alum using the described procedure, except the incubations at 100°C were for 10, 15, 20 and 25 min, respectively. After that, the samples were analyzed by SEC (100 μl) and SDS-PAGE/silver staining (1.7 μg HBsAg per spot).

2.6. Transmission electron microscopy (TEM)

Two drops of HBsAg solution in PBS (0.1 mg/ml) were placed for 5 min onto a 400 mesh copper grid coated with formvar-carbon film. Excess sample was blotted off. Grids were stained with uranyl acetate and examined in a Jeol-JEM 2000EX transmission electron microscope, acceleration voltage 80 kV and magnification 40 000X.

The adsorbed HBsAg was analyzed by sectioning the HBsAg–alum and HBsAg–celite pellets obtained by centrifugation for 10 min at 2500 rpm of the respective preparations (10 ml). Placebo was used as a blank. The pellets were fixed by immersion in 1% glutaraldehyde, rinsed with PBS and dehydrated in increasing (30–100%) ethanol concentrations. The embedding was in Araldite. Each resulting block was sectioned ($N=60$) with an ultramicrotome LKB 2188 (NOVA) and 400-Å sections were mounted on 400 mesh nickel grids without membrane. Staining was with uranyl acetate and lead citrate followed by examination as described.

2.7. Immunoelectron microscopy

The grids coated with soluble HBsAg were floated on six drops of gold buffer (1% BSA in PBS) before transfer to a drop of the PBS-diluted CB Hep1 antibody (dilution, 1:20) for incubation at room temperature (30 min). After washing in gold buffer to remove unbound antibody molecules, the grids were floated on two drops of gold buffer-diluted protein A–gold complexes (dilution, 1:200) for 40 min at room temperature. Finally, the grids were subsequently washed in six drops of gold buffer and two drops of distilled water. After staining with 1% uranyl acetate, the grids were examined as described.

Similarly, the sections ($N=12$) from the placebo, HBsAg–alum and HBsAg–celite pellets were incubated for 5 min on a drop of PBS containing 1% ovalbumin before transfer to a drop of PBS-diluted CB Hep1 monoclonal antibody (dilution 1:20). Incubation was for 60 min at room temperature. The

grids were then rinsed for 5 min with PBS to remove unbound antibody molecules and then incubated on a drop of protein A–colloidal gold complex, pH 7.2, for 40 min at room temperature. Finally, the sections were stained and examined as described.

3. Results and discussion

3.1. Analysis of reduced HBsAg

Recombinant HBsAg is produced by the expression of a 226-amino acid polypeptide in yeast cells where approximately 100 of these polypeptides are assembled intracellularly into 22 nm lipoprotein particles [19]. After purification, the assembled HBsAg particles are detected by SEC, electron microscopy and enzyme-linked immunosorbent assay (ELISA) using polyclonal antibodies [20]. To assess the HBsAg monomer, the particles should be previously reduced. Efficient reduction of HBsAg has been achieved by using a mixture of DTT and mercaptoethanol (DTT/M), instead of one of them alone [21,22], suggesting that these reducing agents do not possess the same reducing power on multiple disulfide bonds within HBsAg particles. Soluble HBsAg–SDS complexes formed after reduction are suitable for further analysis by reversed-phase high-performance liquid chromatography (RP-HPLC) [21] or denaturing SEC [22].

In denaturing SEC (Fig. 1), the reduced HBsAg is resolved into the three peaks: peak 1 corresponds to the co-elution of non-reduced HBsAg and non-protein micellar aggregates, peak 2 to the HBsAg dimers and monomers and peak 3 to lower-molecular-mass non-protein compounds. Earlier studies have shown that peak 1 remaining after DTT/M reduction is produced by non-protein aggregates, probably, by lipid–SDS complexes [22].

The correlation between the areas of peak 2 and the HBsAg concentrations taken for reduction was linear in the range 0.2–1.6 mg/ml HBsAg (r= 0.9991). The reproducibility was tested with three replicate injections of the reduced stock solution of HBsAg on three different days. The relative standard deviations (R.S.D.s) were 1.16–1.36% (within-days) and 1.25–1.65% (between-days).

The presence of shoulders before and after the maximum of peak 2 (Fig. 1) was a hint at the heterogeneity of HBsAg structures formed after reduction. Indeed, as shown by SDS-PAGE/silver staining of SEC-fractions from peak 2 (Fig. 2), the reduced HBsAg was represented by dimers eluting presumably in the forward shoulder, monomers eluting in the maximum of peak 2 and lower-molecular-mass proteins eluting in the backward shoulder.

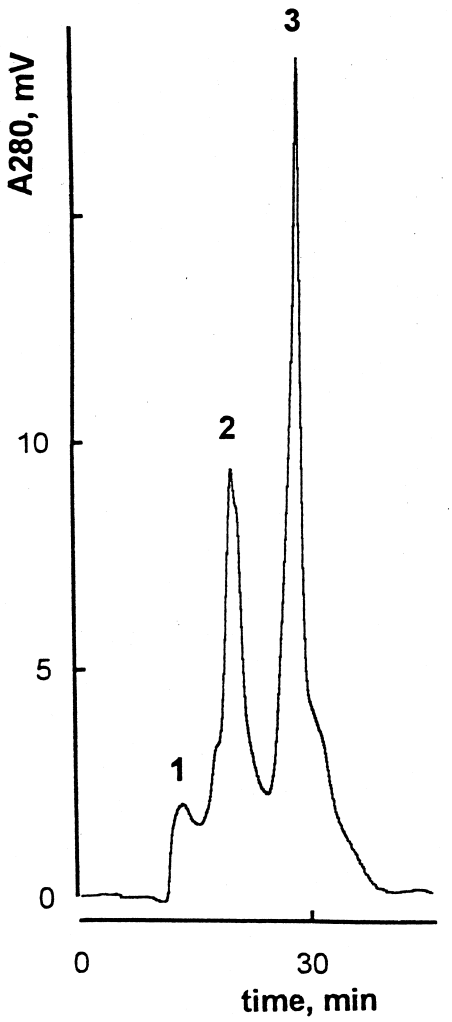

Fig. 1. Chromatogram of reduced HBsAg. Conditions: TSK G4000 SW (600×7.5 mm I.D.); eluent, 0.1 *M* Tris–HCl containing 0.3% SDS, pH 8.0; flow rate, 0.9 ml/min; detection, UV at 280 nm; injection volume, 100 μl; sample buffer, 417 m*M* DTT, 4.2% (w/v) SDS and 16% (v/v) 2-mercaptoethanol. Peaks: 1= Lipid–SDS aggregates, 2=reduced HBsAg, 3=low-molecular-mass non-protein compounds.

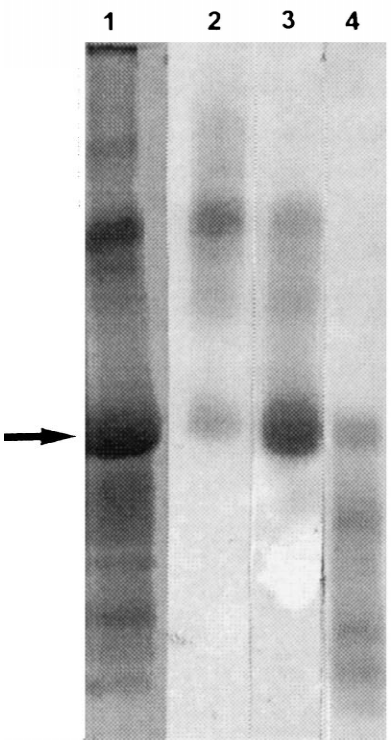

Fig. 2. SDS-PAGE/silver staining of DTT/M-reduced HBsAg (lane 1) subjected to SEC fractionation (lanes 2–4): forward shoulder of peak 2 (lane 2), maximum of peak 2 (lane 3) and backward shoulder of peak 2 (lane 4). Experimental conditions as in text. The arrow indicates the M_r 24 000 HBsAg monomer. Amount, 20 (lane 1) and 1.7 (lanes 2–4) μg HBsAg.

The last ones migrated before the M_r 24 000 monomer band on SDS-gel (Fig. 2, lane 4) and were recognized in immunoblotting (data not shown). When HBsAg monomer from the maximum of peak 2 (Fig. 2, lane 3) was repeatedly reduced, no appearance of lower bands was detected evidencing that the observed lower bands are not generated by the reducing procedure. We assumed these bands as degradation products. Similar degradation bands were detected by immunoblotting of HBsAg expressed in *S. cerevisiae* or *H. polymorpha* [23]. Since these bands were found not only in purified material but also in crude HBsAg-containing yeast extract [23], the detected degradation probably takes place in vivo. The degradation products are particle-associated, because we could not separate them from assembled particles by SEC under non-denaturing conditions [data not shown]. Since HBsAg particles are resistant to proteases [24], the degradation probably implies covalent modifications of labile amino acids exposed on particle surface (Ser, Thr β-elimination and racemization, Asn deamidation, Cys, Trp, Tyr oxidation or the hydrolysis of peptide bonds [25]).

3.2. Analysis of desorbed HBsAg

To improve the immunogenicity of purified HBsAg particles, these are adsorbed onto aluminium hydroxide gel in hepatitis B vaccine. Like tetanus toxoid and diphtheria toxoid [9], HBsAg is adsorbed on alum independently on pH and excess phosphate ions, and this adsorption is irreversible under non-denaturing conditions [unpublished results]. In the present work, adsorbed HBsAg was recovered after the reduction of HBsAg–alum pellet with a mixture of 0.4 *M* Na/PO_4, pH 8.0–DTT/M sample buffer (Fig. 3). The desorbed protein migrated presumably as a M_r 24 000 monomer onto SDS-gel. When the known amounts of HBsAg were reduced and applied on gel, the intensities of the M_r 24 000-bands detected by laser densitometry were linearly related to the HBsAg amounts ($r=0.995$). By extrapolating the intensity of the band from the desorbed sample, the HBsAg recovery was estimated to be $43\pm4\%$. This value may be overestimated due to a significant enlargement of the band from desorbed HBsAg compared to those from HBsAg solutions (Fig. 3). As an alternative, the desorbed HBsAg was determined by SEC. The chromatogram of desorbed HBsAg was quite similar to that of HBsAg reduced in solution (Fig. 4). By plotting the area of peak 2 from the desorbed sample on the calibration curve, the HBsAg recovery was calculated to be $50\pm1\%$. Hence, both SDS-PAGE and SEC indicate that a large portion of adsorbed HBsAg cannot be recovered under reducing conditions.

In respect to the recoverable fraction of HBsAg, it was continuously degraded at increasing the rates of reduction in the range from 3 to 25 min. In the chromatogram of desorbed HBsAg, the height of peak 2 was gradually diminished, whereas the backward shoulder corresponding to the elution of degraded polypeptides increased. After 20 min of boiling, the desorbed HBsAg was presented mainly as the protein fragments. Under the same conditions,

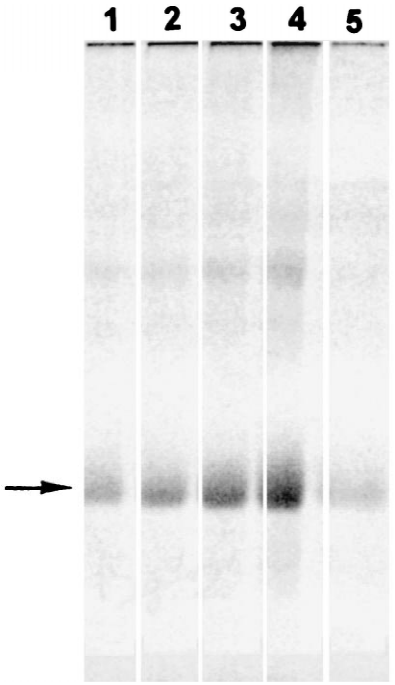

Fig. 3. SDS-PAGE/Coomasie blue staining of HBsAg standard solutions (lanes 1–4) and alum-desorbed sample. Experimental conditions as in Section 2. The arrow indicates the M_r 24 000 HBsAg monomer. Amount, 15 (lane 1), 20 (lane 2), 25 (lane 3) and 30 (lane 4) μg HBsAg. Desorbed sample: the value expected assuming the complete recovery of HBsAg, 20 μg; the value calculated from the calibration curve, 9 μg.

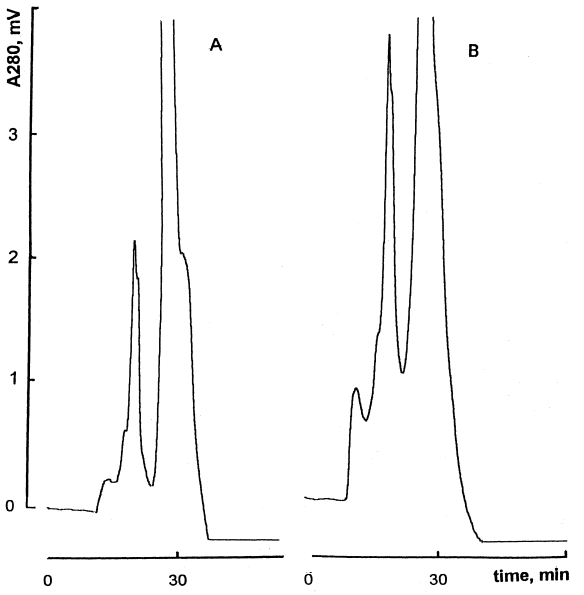

Fig. 4. Chromatogram of HBsAg reduced in solution (A) and desorbed from alum under reducing conditions (B). Conditions as in Fig. 1; concentration, 0.5 mg/ml HBsAg (A); injection volume, 100 μl. Desorbed HBsAg: the value expected, assuming complete HBsAg recovery, 0.5 mg/ml HBsAg; the value calculated from the calibration curve, 0.24 mg/ml HBsAg.

the HBsAg monomer from intact particles was stable and no changes in its chromatographic profile (Fig. 1) were observed even after 30 min of boiling with DTT/M sample buffer. The degradation detected by SEC for the recoverable fraction of adsorbed HBsAg was almost undetectable by SDS-PAGE, where larger rates of boiling led to a weak increase in the intensity of degradation bands (Fig. 5, right). This is probably due to a highly intensive, selective staining of HBsAg bands compared to that of degradation bands.

In conclusion, the present study of HBsAg desorption raised two important observations. First, only half protein adsorbed is recovered under reducing conditions. Since the reducing conditions are capable to efficiently disrupt any type of interactions having these an ionic, hydrophobic and/or ligand-exchange nature, the non-recoverable fraction of HBsAg should be trapped to alum by an additional, besides adsorption, mechanism making protein molecules inaccessible to reducing buffer. If the particulate structure of HBsAg were to be preserved in the adsorbed state, the HBsAg monomers would be quantitatively recovered. Second, the fraction of HBsAg recoverable under reducing conditions is prone to temperature-induced degradation, unlike intact HBsAg. Since the stability of a protein is determined by its three-dimensional structure [25], the results indicate that the structure of HBsAg particles is altered by alum adjuvant.

The increasing attention to particulate polymeric antigens in the form of virus-like particles is related to their ability to induce specific, cell-mediated immune response in the absence of adjuvants [Reviews, 26, 27]. Cytotoxic T lymphocytes (CTLs) provide a critical arm of the immune system in eliminating autologous cells expressing foreign antigen [28–30]. Although the mechanisms by which these approaches lead to the induction of CTLs are

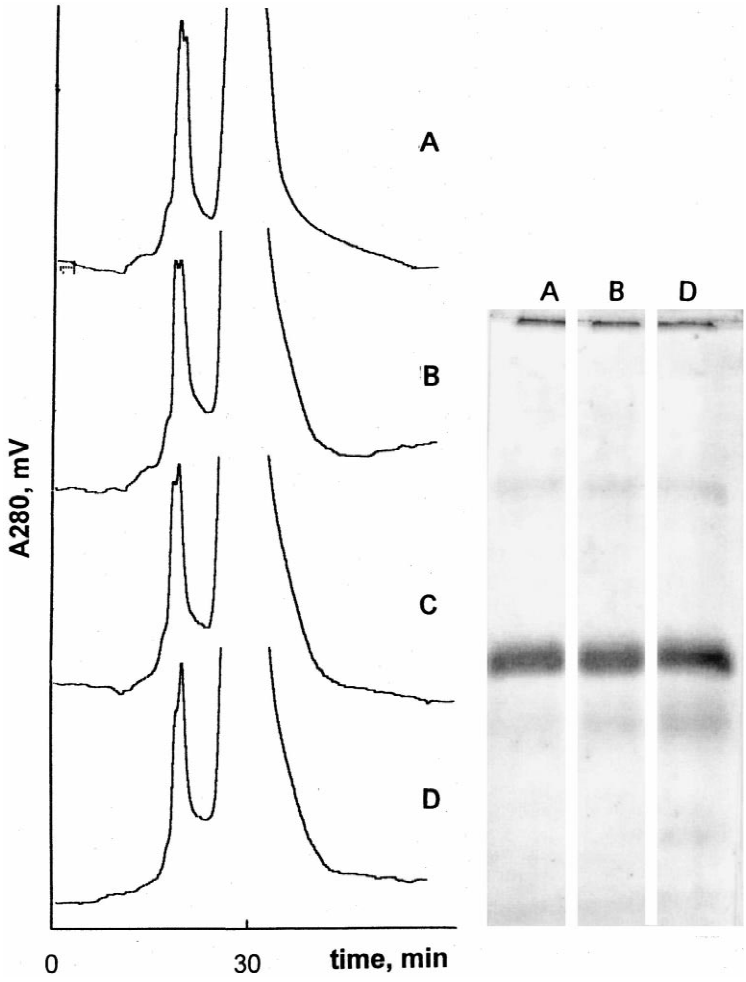

Fig. 5. Chromatographic profile (left) and SDS-PAGE/silver staining pattern (right) of desorbed HBsAg after 10 (A), 15 (B), 20 (C) and 25 (D) min of boiling the HBsAg–alum pellet with DTT/M buffer. Chromatographic conditions as in Fig. 1; injection volume, 100 μl. Electrophoretic conditions as in Section 2; amount, 1.7 μg HBsAg.

unknown, it has been suggested that the particulate nature of virus-like particles favors their optimal delivery to the class I antigen presentation pathway [11,12,31]. Unexpectedly, particulate antigens, including HBsAg, failed to stimulate CTLs after their adsorption on alum eliciting, in contrast, substantial antibody titers [10, 11]. Hence, a supposition has been made that the particulate structure of virus-like particles may be compromised by the adsorption on adjuvant [31]. Our results from SEC and SDS-PAGE support this feeling. In order to provide a direct evidence for the loss of particulate structure of HBsAg on alum, we analyzed the HBsAg–alum preparation by immunoelectron microscopy.

3.3. Immunoelectron visualization of adsorbed HBsAg

The intact HBsAg was seen in electron microscope as 22-nm spheres (Fig. 6A). After its adsorption on alum, no particles were found in the HBsAg–alum sections suggesting alterations in the HBsAg morphology (Fig. 6B). In a few sections, a structures were found resembling HBsAg particles,

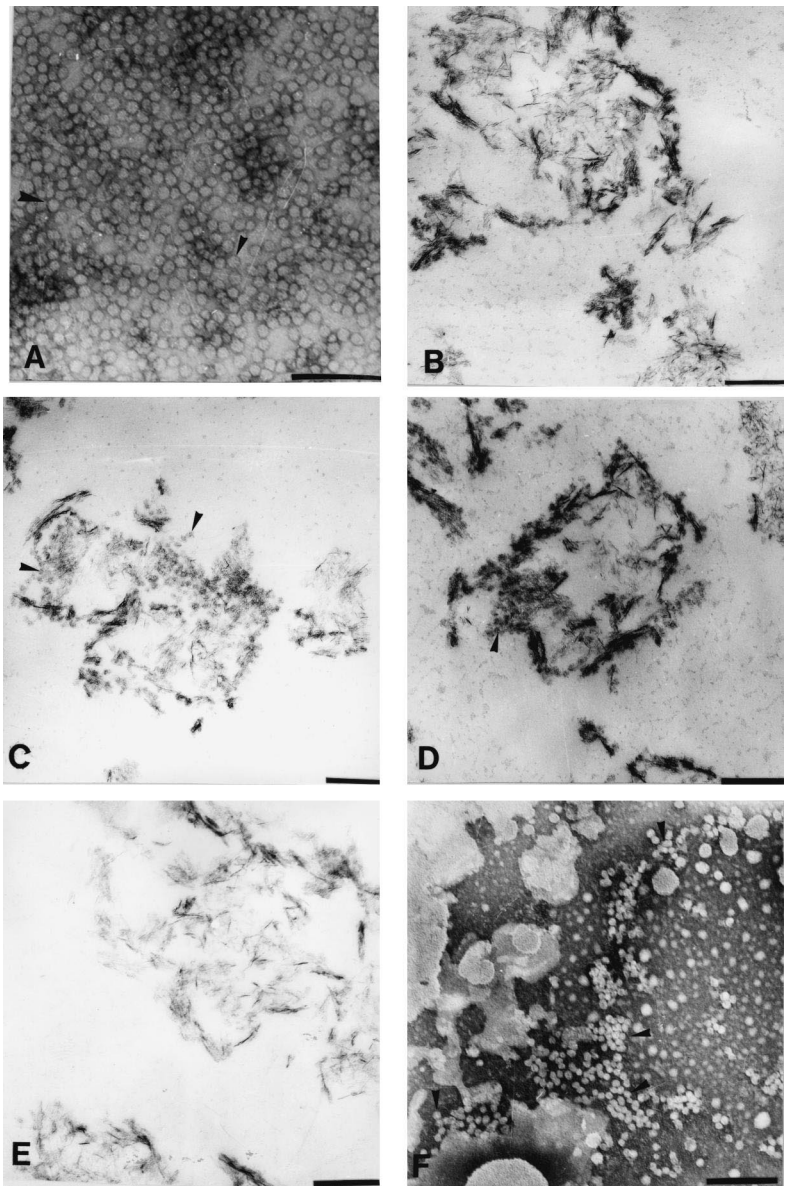

Fig. 6. Electron micrographs of intact HBsAg (A), HBsAg–alum sections (B, C and D), placebo (E) and HBsAg–alum (F) sections. Experimental conditions as in Section 2. Scale bar is 200 nm.

but with a defect in particulation, suggesting particle damage (Fig. 6C and D). These structures were absent in the placebo sections (Fig. 6E). In order to prove that HBsAg structure is unaffected under the conditions of analysis, the HBsAg was adsorbed on celite and the HBsAg–celite sections were prepared as described. The HBsAg adsorption on celite is reversible [14], thus, the HBsAg particles should be found in the HBsAg–celite sections. As expected, the HBsAg particles retained in the pores of celite were clearly visualized (Fig. 6F). The adsorbed HBsAg, undetectable by direct visualization, was

identified here by immunoelectron microscopy (IEM) using CB Hep1 monoclonal antibody. One of the most interesting aspects of this approach is its potential to detect HBsAg independently on the state of folding. When the HBsAg–alum sections were incubated with CB-Hep 1 antibody followed by successive labeling with protein A–gold complex, these were specifically labeled proving thus the presence of HBsAg on alum gel (Fig. 7A and B). The HBsAg appeared as in a dark-staining matrix structure of $Al(OH)_3$ (Fig. 7A) as in the gel pores (Fig. 7B). It is essential that non-specific adsorption of gold on alum was minimal in the absence of HBsAg (Fig. 7C).

In IEM of intact HBsAg, the mapping of 15-nm gold onto 22-nm HBsAg particles produces a labeling pattern characterized by the presence of hoops around gold particles (Fig. 7D). This pattern was not observed after immunolabeling of HBsAg–alum sections (Fig. 7A and B) proving once more the loss of particulate structure of HBsAg after adsorption on alum.

3.4. Proposed model

The initial adsorption event is a function of the interfacial activity of various groups on a particle surface and on the adsorbent [32]. The active sites on alum are ascribed to aluminium ions (Lewis acids) or hydroxyls [7], whereas those on HBsAg particle are represented by water-exposed phospholipids and hydrophilic protein domains [33]. The HBsAg–alum interaction is of non-ionic character, because it is insensitive to the conditions of pH and ionic strength. Despite ionic interaction, proteins are adsorbed on alum by hydrophobic [34] and ligand-exchange [35,36] forces. The last mechanism comprises the chemisorptive binding of phosphate and carboxylate groups of a protein to alum surface in accord with the Lewis acid–base model. Taking into

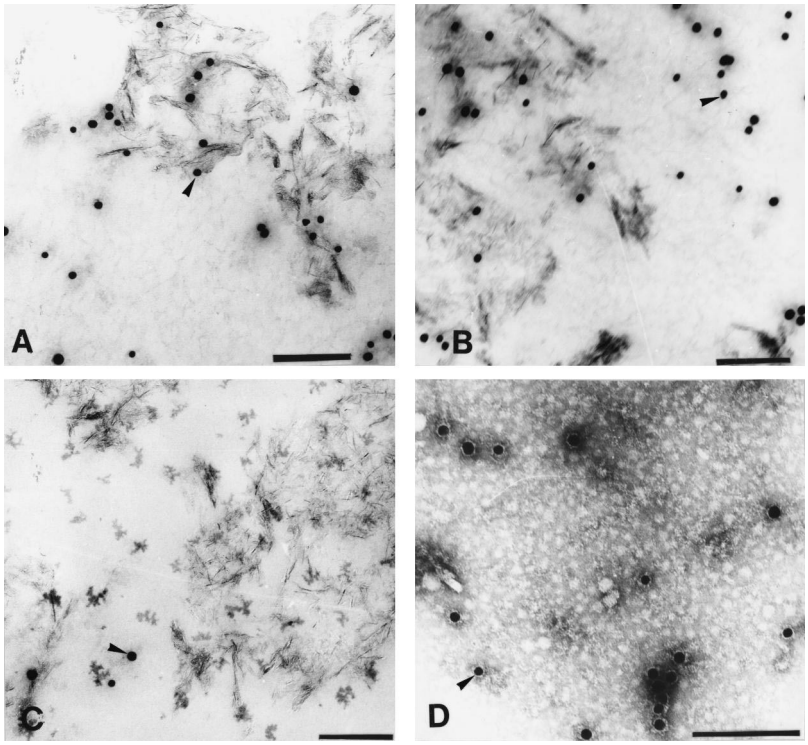

Fig. 7. Protein A–gold electron microscopic localization of HBsAg on alum (A, B). Non-specific labeling of alum in the absence of HBsAg (C). Immunolabeling pattern of intact HBsAg (D). Experimental conditions as in Section 2. Scale bar is 200 nm.

account that phosphate is one of the strongest Lewis bases, the interaction of phosphate heads from phospholipids of HBsAg with unsaturated aluminium ions is highly expected. Phospholipids are the predominant lipid structures within HBsAg particles [37] and play a crucial role in the particle stabilization [38]. The lipid–protein interactions are responsible for the formation of the proper helical structure of the HBsAg protein, which disposes the remainder of the protein on the surface or interior of the particle. The lipid–protein interactions stabilize the conformation of the exterior hydrophilic regions which contain the HBsAg antigenic sites [38]. Hence, the adsorption of phospholipids on alum is expected to produce a damage of integrity of outer lipid monolayer followed by rearrangements in hydrophobic protein domains and lipid core inside the HBsAg particle. According to this model, the observed low recovery of HBsAg under reducing conditions can be explained by a trap of the non-recoverable protein monomers between alum and disordered lipids from lipid core. On the other hand, the alterations in lipid–protein interactions within HBsAg particle destabilize α-helices by the exposure of protein domains previously buried in lipid bilayer [38]. Being less stable, the conformationally altered HBsAg monomers are more sensitive to degradation that explains the observed temperature-induced degradation of the recoverable HBsAg monomers.

Acknowledgements

We thank M.C. de la Rosa for excellent technical assistance in electron microscopic experiments and J. Seoane for the reproduction of electron micrographs.

References

[1] from Hepatitis Weekly, July 8 (1996) 1.
[2] W. Jilg, F. Deinhardt, J. Infect. 13 (1986) 47.
[3] W. Jilg, B. Lorbeer, M. Schmidt, B. Wilske, G. Zoulek, F. Deinhardt, Lancet 11 (1984) 1174.
[4] F. Lugoboni, S. Migliozzi, F. Schiesari, N. Pauletto, G.L. Bovo, S. Ciaffoni, P. Mezzelani, Vaccine 15 (1997) 1014.
[5] R.M. Zinkernagel, S. Ehl, P. Aichele, S. Oehen, T. Kundig, H. Hengartner, Immunol. Rev. 156 (1997) 199.
[6] R.P. Weissburg, P.W. Berman, J.L. Cleland, D. Eastman, F. Farina, S. Frie, A. Lim, J. Mordenti, M.R. Peterson, K. Yim, M.F. Powell, Pharm. Res. 12 (1995) 1439.
[7] S.L. Hem, J.L. White, in: M.F. Powell, M.J. Newman (Eds.), Vaccine Design: The Subunit and Adjuvant Approach, Plenum Press, New York, 1995, p. 249.
[8] S.L. Hem, J.L. White, J. Parenteral Sci. Tech. 38 (1984) 2.
[9] R.K. Gupta, B.E. Rost, E.H. Relyveld, G.R. Siber, in: M.F. Powell, M.J. Newman (Eds.), Vaccine Design: the Subunit and Adjuvant Approach, Plenum Press, New York, 1995, p. 229.
[10] R. Schirmbeck, K. Melber, T. Mertens, J. Reimann, Eur. J. Immunol. 24 (1994) 1088.
[11] G.T. Layton, S.J. Harris, A.J. H. Gearing, M. Hill-Perkins, J.S. Cole, J.C. Griffiths, N.R. Burns, A.J. Kingsman, S.E. Adams, J. Immunol. 151 (1993) 1097.
[12] S.J. Harris, S.A. Woodrow, A.J. H. Gearing, S.E. Adams, A.J. Kingsman, G.T. Layton, Vaccine 14 (1996) 971.
[13] E. Pentón, Eur. Pat. Publ. No. EP 480525 (1992).
[14] A. Agráz, Y. Quiñones, N. Expósito, F. Breña, J. Madruga, E. Pentón, L. Herrera, Biotechnol. Bioeng. 42 (1993) 1238.
[15] U.K. Laemmli, Nature 227 (1970) 680.
[16] W. Wray, T. Boulikas, V.P. Wray, R. Hancock, Anal. Biochem. 118 (1981) 197.
[17] O. Rodriguez, M. Izquierdo, Y. Martinez, A. Garcia, Adv. Biotecnol. Moderna 2 (1994) 64.
[18] O.H. Lowry, N.J. Rosebrough, A.L. Farr, R.J. Randall, J. Biol. Chem. 265 (1951) 265.
[19] P. Valenzuela, A. Medina, W.J. Rutter, G. Ammerer, B.D. Hall, Nature 298 (1982) 347.
[20] D. Tleugabulova, J. Reyes, L. Costa, J. Díaz, J.J. Madrazo-Piñol, Chromatographia 45 (1997) 317.
[21] D.O. O'Keefe, A.M. Paiva, Anal. Biochem. 230 (1995) 48.
[22] D. Tleugabulova, J. Chromatogr. B 713 (1998) 401.
[23] Z.A. Janowicz, K. Melber, A. Merckelbach, E. Jacobs, N. Harford, M. Comberbach, C.P. Hollenberg, Yeast 7 (1991) 431.
[24] R. Prange, R.E. Streeck, EMBO J. 14 (1995) 247.
[25] S. Li, Ch. Schoneich, R. Borchardt, Biotech. Bioeng. 48 (1995) 490.
[26] S.C. Gilbert, M. Plebanski, S.J. Harris, C.E.M. Allsopp, R. Thomas, G.T. Layton, A.V.S. Hill, Nature Biotechnol. 15 (1997) 1280.
[27] P.D. Robbins, H. Tahara, S.C. Ghivizzani, Trends Biotechnol. 16 (1998) 35.
[28] Y.L. Lin, B.A. Askonas, J. Exp. Med. 154 (1981) 225.
[29] M.M. McNeal, K.S. Barone, M.N. Rae, R.L. Ward, Virology 214 (1995) 387.
[30] P. Reusser, S.R. Riddell, J.D. Meyers, P.D. Greenberg, Blood 78 (1991) 1373.
[31] C. Sedlik, M.F. Saron, J. Sarraseca, I. Casal, C. Leclerc, Proc. Natl. Acad. Sci. USA 94 (1997) 7503.
[32] J.D. Andrade, V. Hlady, A.P. Wei, C.G. Golander, Croatica Chem. Acta 63 (1990) 527.
[33] M. Sato, Y. Sato-Miyamoto, K. Kameyama, N. Ishikawa, M. Imai, Y. Ito, T. Takagi, J. Biochem. 118 (1995) 1297.

[34] A. Bhaduri, N. Matsudomi, K.P. Das, Biosci. Biotech. Biochem. 60 (1996) 1559.
[35] R.J. Sepelyak, J.R. Feldkamp, T.E. Moody, J.L. White, S.L. Hem, J. Pharm. Sci. 73 (1984) 1514.
[36] M.J. Gorbunoff, Anal. Biochem. 136 (1984) 425.
[37] F. Gavilanes, J.M. Gonzalez-Ros, D. Peterson, J. Biol. Chem. 257 (1982) 7770.
[38] F. Gavilanes, J. Gomez-Gutierrez, M. Aracil, J.M. Gonzalez-Ros, J.A. Ferragut, E. Guerrero, D. Peterson, Biochem. J. 265 (1990) 857.